Journal of Biomedical Optics

BiomedicalOptics.SPIEDigitalLibrary.org

Assessment of intraocular pressure sensing using an implanted reflective flexible membrane

Andrey Nazarov
Boris Knyazer
Tova Lifshitz
Mark Schvartzman
Ibrahim Abdulhalim

SPIE.

Andrey Nazarov, Boris Knyazer, Tova Lifshitz, Mark Schvartzman, Ibrahim Abdulhalim, "Assessment of intraocular pressure sensing using an implanted reflective flexible membrane," *J. Biomed. Opt.* **22**(4), 047001 (2017), doi: 10.1117/1.JBO.22.4.047001.

Assessment of intraocular pressure sensing using an implanted reflective flexible membrane

Andrey Nazarov,[a,*] Boris Knyazer,[b] Tova Lifshitz,[b] Mark Schvartzman,[c] and Ibrahim Abdulhalim[a]
[a]Ben-Gurion University of the Negev, Ilse Katz Institute for Nanoscale Science and Technology, Department of Electro-Optic Engineering, Beer-Sheva, Israel
[b]Ben-Gurion University of the Negev, Soroka University Medical Center, Department of Ophthalmology, Beer-Sheva, Israel
[c]Ben-Gurion University of the Negev, Department of Material Engineering, Beer-Sheva, Israel

Abstract. Glaucoma is a neurodegenerative condition that is the leading cause of irreversible blindness worldwide. Elevated intraocular pressure (IOP) is the main cause for the development of the disease. The symptoms of this form, such as deterioration of vision and scotomas (loss of visual fields), appear in the latter stages of the disease. Therefore, an IOP monitoring device is needed for better, simpler, and faster diagnosis, and to enable a fast treatment response. We present a theoretical assessment as well as preliminary experimental results of a simple approach for easy, optical, IOP self-monitoring. It is based on a polydimethylsiloxane membrane coated with a reflective layer and a Hartmann–Shack wavefront sensor. Nearly linear correlation is found between membrane deformation and Zernike coefficients representing defocus primary spherical aberration, with high sensitivity and negligible dependence on the measurement distance. The proposed device is expected to provide an accurate IOP measurement resolution of less than ± 0.2 mm Hg with a pressure dependence on working distances <0.7 mm Hg/cm for a thick membrane; the corresponding values for a thin membrane are ± 0.45 mm Hg and <0.6 mm Hg/cm, respectively, at typical IOP values—up to 40 mm Hg. [DOI: 10.1117/1.JBO.22.4.047001]

Keywords: intraocular pressure; polydimethylsiloxane; flexible membrane; wavefront sensor; intraocular pressure self-monitoring.

Paper 160516RRR received Jul. 26, 2016; accepted for publication Mar. 16, 2017; published online Apr. 5, 2017.

1 Introduction

Glaucoma is a group of eye diseases related to elevated intraocular pressure (IOP) and is the second most common cause of blindness worldwide, after cataracts. Glaucoma, which may lead to irreversible blindness, affects tens of millions of people worldwide each year.[1] A previous research[2] showed that the global prevalence of glaucoma for populations of the ages 40 to 80 years is 3.54%. In 2013, it was estimated that 64.3 million people worldwide from the ages of 40 to 80 suffer from glaucoma and these numbers are expected to increase to 76 million in 2020 and 111.8 million in 2040.[2] In 2010, out of 60 million suffering from glaucoma, about 8.4 million became blind because of the disease.[3]

IOP is determined by the difference between formation and drainage of the aqueous humor. For instance, blockage in the aqueous humor drainage can result in elevated IOP. Elevated IOP is considered to be the main cause of glaucoma and is, therefore, used for its diagnosis. The most common and accepted way for measuring IOP is by using a Goldmann tonometer. The use of a Goldmann tonometer has its own drawbacks since this technique is invasive, uncomfortable, and requires the application of anesthesia to the numb eye in order to prevent eye reflexes. Additionally, this measurement requires a skilled technician or an ophthalmologist.[4] IOP measurement using a Goldmann tonometer may result in a misdiagnosis unless the central corneal thickness measurement is taken into account. Due to the complexity of the measurement procedure, IOP measurements are commonly performed only few times a year—not as frequently as they should be for proper treatment of glaucoma. A monitoring device for proper tracking of the IOP is needed for better, simpler, and faster diagnosis and to enable fast treatment response.

Several wireless IOP measurement devices were proposed. Some of them are based on measuring the change of capacitance of the measuring device caused by the IOP changes,[5] while others use microelectromechanical systems-based pressure sensor.[6–8] A strain gauge has also been suggested to be embedded in a standard contact lens and used for IOP measurement.[9] All these devices require an external unit to measure and supply power. In addition, optical methods were also achieved by using a photonic crystal membrane,[10] localized surface plasmon resonance in metal nanorods,[11] photonic crystal slabs,[12] and spectroscopic response from gold (Au) nanoparticles;[13] these devices are not capable of operating without a power source or they require a nondirect observation of a phenomenon, such as plasmon resonance or spectroscopic data. Our proposed device is much simpler since it is based on a simple phenomenon of light reflection and wavefront deformation that is easy to measure and process.

In this work, we propose and demonstrate an approach for measuring IOP by using the mechanical properties of a flexible reflective polydimethylsiloxane (PDMS) membrane implanted into the anterior chamber (AC) or partially into the cornea and a wavefront sensor, which can characterize the deformation in the reflected wavefront. The implantation of the membrane in the cornea will be done to patients who suffer from glaucoma

*Address all correspondence to: Andrey Nazarov, E-mail: andreyn@post.bgu.ac.il

1083-3668/2017/$25.00 © 2017 SPIE

and especially primary open angle glaucoma (POAG). The patients with POAG suffered from elevated IOP and did not usually suspect it. Currently, clinicians rely on a single "snap-shot" measure of IOP or a maximum of 3 to 4 "snap-shot" readings of measure that are performed during the patient's visit at the ophthalmologist's clinic. It is well known that IOP is predisposed to fluctuations during the day and due to several activity conditions (tight tie, Valsalva's maneuver, holding breath, change of position, hormonal status, and etc.).[14] These daily activities frequently create difficulties for ophthalmologists for accurate follow-up. Therefore, constant IOP monitoring is critical in understanding and following up the progression of glaucomatous patients. Until now, there has been no available technology that enables continuous measurement of the IOP; hence implantation of a PDMS membrane to a patient's cornea will provide precise information about fluctuations of IOP and progression of glaucoma. This is the motivation for the presented work here.

2 Simulations

The proposed device is designed to be implanted into the AC and attached to the corneal surface without damaging the field of view of the patient. The PDMS membrane can be prepared using a Sylgard® 184 silicone elastomer kit by Dow Corning and coated using two metal layers—titanium (Ti) and Au or silver (Ag).

A plane wave incident on the reflective deformed membrane will reflect with a distortion governed by the deformation of the membrane, which can be measured using a Hartmann–Shack (HS) wavefront sensor and translated to the IOP. The device is simple and accurate for self-monitoring of patients at risk.

Figure 1 describes the placement of the device in the AC. The mean AC width is 12.53 ± 0.47 mm and the mean AC depth is 2.99 ± 0.323 mm.[15] Maximum pupil diameter is 8 mm, therefore, the device could not be more than 2 mm in diameter (w) while its thickness (t) may be as large as 2 mm. It is important to understand the effect of the volume change upon the membrane deformation on the eye inner pressure. This problem may be overcome by increasing the size of the inner cell and thus reducing the effect of pressure rising in the inner cavity. For example, the cell may be elongated and by extending the wall (in the z-direction in Fig. 1) of the cell such that the functionality of the device will remain the same without any effect on the vision. This will allow reduction of the inner cavity pressure changes due to membrane deformation. Alternatively, the cell can include a cavity between the membrane and a solid surface facing the cornea so that the volume change will be absorbed in that cavity.

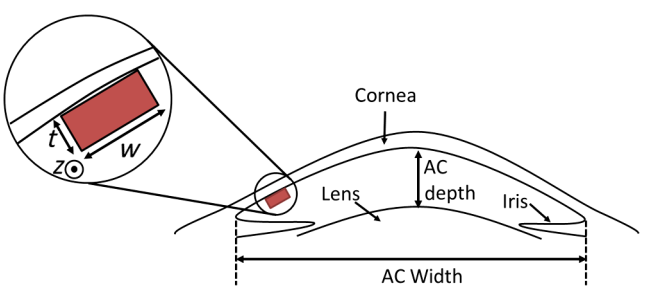

Fig. 1 Schematic showing the proposed placement of the device in the AC, t and w are the thickness and width of the proposed device, respectively. It can be attached to the cornea or implanted partially inside the cornea.

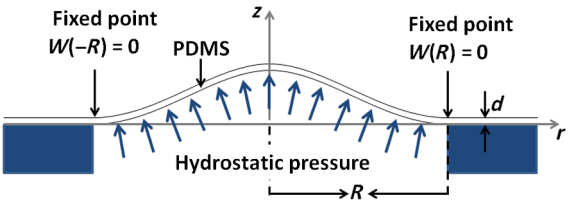

Fig. 2 Schemtic of the geometry of a flexible membrane clamped at its edges under hydrostatic pressure.

2.1 *Deformation of the Polydimethylsiloxane Flexible Membrane*

The deformation of a circular clamped membrane under hydrostatic pressure is described fully by a set of two nonlinear differential equations [16,17] and the geometry described in Fig. 2

$$\frac{d^2u}{dr^2}+\frac{1}{r}\frac{du}{dr}-\frac{u}{r^2}=-\frac{1-\nu}{2r}\left(\frac{dw}{dr}\right)^2-\frac{dw}{dr}\frac{d^2w}{dr^2}$$
$$\frac{d^3w}{dr^3}+\frac{1}{r}\frac{d^2w}{dr^2}-\frac{1}{r^2}\frac{dw}{dr}=\frac{12}{d^2}\frac{dw}{dr}\left[\frac{du}{dr}+\nu\frac{u}{r}+\frac{1}{2}\left(\frac{dw}{dr}\right)^2\right]+\frac{pr}{2F}, \tag{1}$$

having the boundary conditions

$$\begin{cases} u=\frac{dw}{dr}=0, & \text{at } r=0 \\ u=w=\frac{dw}{dr}=0, & \text{at } r=R \end{cases}, \tag{2}$$

where $u(r)$ and $w(r)$ are the displacements in the radial and axial directions r and z, respectively, d is the thickness of the membrane, and p is the uniform hydrostatic pressure. The flexural rigidity of the axisymmetric membrane is expressed as $F = E \cdot d^3/[12(1-\nu^2)]$, where E and ν are the Young's modulus and Poisson's ratio, respectively.

Figure 3 presents PDMS membrane deformation profiles for various pressure values with $E = 1.12$ (MPa), $\nu = 0.48$,[17] thickness $d = 500$ (μm), and radius $R = 5000$ (μm), obtained by COMSOL Multiphysics.

It is useful to describe the deformation of the membrane as a radially symmetric aspherical surface. In this case, $w(r)$ can be expressed as

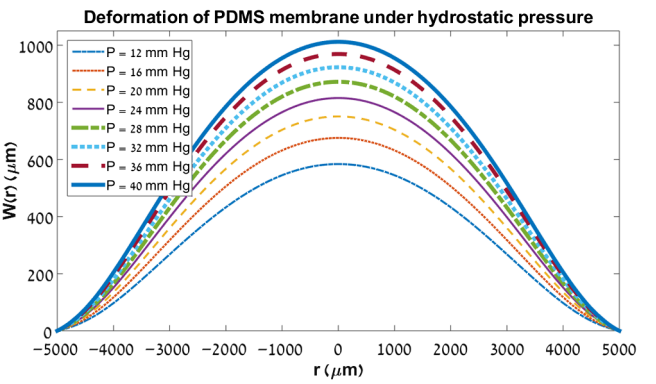

Fig. 3 Deformation of a PDMS membrane with $E = 1.12$ (MPa), $\nu = 0.48$, $d = 500$ (μm), and $R = 5000$ (μm) for pressures in the range of 12 to 40 mm Hg.

$$w(r) = \frac{cr^2}{1 + \sqrt{1 - (1+K)c^2r^2}} + \sum_{k=2}^{\infty} a_k r^{2k}, \tag{3}$$

where c is the vertex curvature, K is the conic constant of the profile, and a_k is the aspheric coefficient. Since the membrane is clamped at its edges, the curve that most resembles the deflected shape is a parabola, therefore, it is safe to assume that the conic constant is $K = -1$ for this case, and only the aspheric coefficient a_k is needed for fully describing the deformed membrane.

2.2 *Wavefront Distortion Simulation*

A plane wave incident on a reflective deformed membrane will reflect with a distortion governed by the deformation of the membrane. For this task, the membrane deformation for various pressures was fitted to Eq. (3) to acquire the aspherical coefficients up to the 10th power of r. First, Eq. (3) was used to find the aspherical coefficients of the deformed membrane and these were used for simulating a reflective aspherical surface in optics software for layout and optimization (OSLO). Second, a simulation describing a plane wave reflected from an aspherical surface was performed and analyzed using Zernike polynomials for the wavelength of 632.8 nm. Since the device will ideally be placed near the cornea, another surface was added to the simulation to represent the cornea. Figure 4 illustrates the simulated surfaces. Table 1 lists the different regions used in the simulation, their radii of curvature, and refractive indices.

2.3 *Zernike Decomposition*

Zernike polynomials are commonly used for the description and decomposition of wavefront distortions. Using Zernike polynomials, the wavefront is decomposed into basic wavefront distortion types represented by a specific Zernike polynomial, allowing quantification of the magnitude of each distortion and assessing the contribution of each element in the optical system, which may introduce distortions to the shape of the emerging wavefront.

We used OSLO for simulating the effect on a plane wave, which can also decompose the reflected wavefront to Zernike polynomials. Four radial polynomials presented notable contributions to the distorted reflected wavefront: $R_0^0(r)$, $R_2^0(r)$, $R_4^0(r)$, and $R_6^0(r)$. Only these radial polynomials are considered, since the simulation is for normal incidence and the system is radially symmetric. All other Zernike polynomials gave null results and therefore are not shown here. These four radial polynomials describe piston, defocus, primary, and secondary spherical aberrations, respectively.

2.4 *Simulation Results*

The simulation was performed twice, once for a membrane with $d = 500\,(\mu\text{m})$ and $R = 5000\,(\mu\text{m})$, which are the dimensions of the fabricated membrane and are restricted by the measurement setup. The second simulation was performed for $d = 100\,(\mu\text{m})$ and $R = 1000\,(\mu\text{m})$. The dimensions in the later simulation are the desirable dimensions for the final implanted device.

We will present the theoretical study for all four contributing polynomials in two cases, thick and thin membranes, and find which polynomials may be used for IOP measurement.

2.4.1 *Thick membrane case*

Simulation results for the four significant polynomials mentioned in Sec. 2.4 are described in Fig. 5. To use a specific

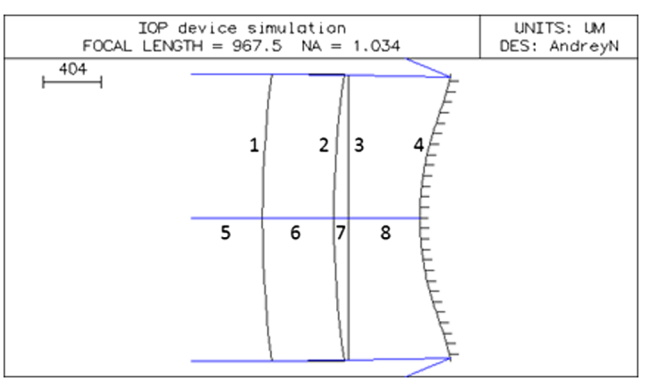

Fig. 4 Surfaces simulated in OSLO-EDU. The different surfaces are described in Table 1.

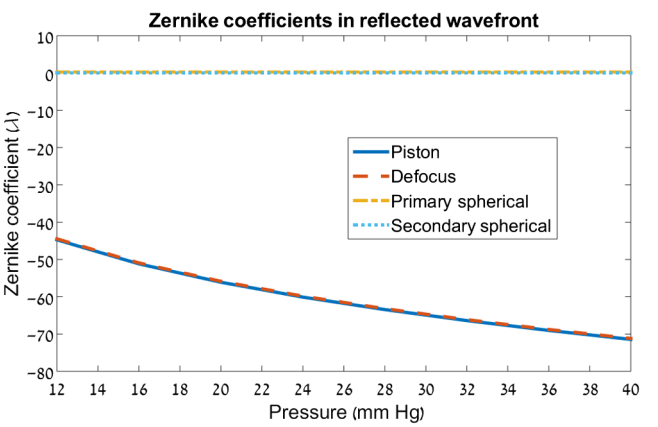

Fig. 5 Zernike coefficients for $R_0^0(r)$, $R_2^0(r)$, $R_4^0(r)$, and $R_6^0(r)$ (corresponding to piston, defocus, primary spherical, and secondary spherical, respectively) in the reflected wavefront for pressure changes in the range of 12 to 40 mm Hg.

Table 1 List of the simulated surfaces, regions, and their specifications.

Surface No.	Surface	Radius of curvature	Region No.	Region	Refractive index
1	Front corneal surface	7.7 mm	5	Air	1
2	Back corneal surface	6.8 mm	6	Cornea	1.376
3	Rigid flat substrate	Infinity	7	Aqueous humor	1.336
4	Reflective PDMS membrane	Aspherical reflective membrane	8	Air	1

Zernike coefficient, two conditions are needed to be constant: monotonic behavior and a small change of measurement distance. Out of the four polynomials, the first two $[R_0^0(r), R_2^0(r)]$ are greatly affected by pressure and they change with the measurement distance, wherein the last two polynomials $[R_4^0(r), R_6^0(r)]$ hardly change with the deformation of the membrane or when the pressure changes.

The behavior of the Zernike coefficient for defocus is described in Fig. 6. The monotonic behavior of $R_0^0(r)$ and $R_2^0(r)$ suggests that the IOP can be estimated directly by measuring these two Zernike coefficients.

Figure 7 describes the Zernike coefficients' distance dependence for various pressures. For the first two coefficients $R_0^0(r)$ and $R_2^0(r)$, the slope of the change is in the range of 0.38 to 0.4 λ/cm for all pressure values, while for $R_4^0(r)$ and $R_6^0(r)$, the slope is at least 2 orders of magnitude smaller and changes slightly between different pressure values.

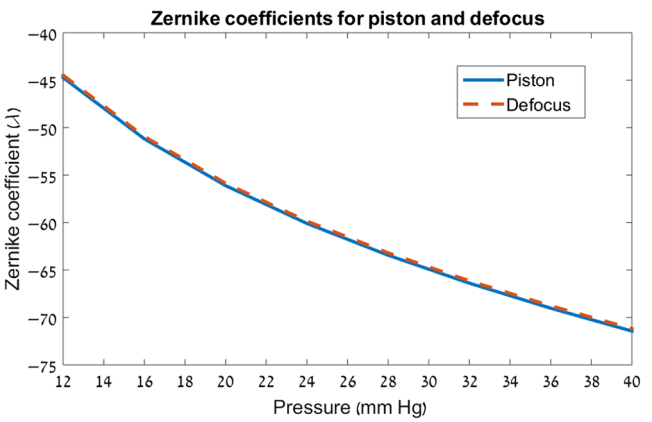

Fig. 6 Zernike coefficient for piston and defocus in the range of 12 to 40 mm Hg.

To quantify the simulation results and find the accuracy of the proposed device, an understanding of the accuracy and sensitivity of the wavefront sensor suitable to measure the Zernike coefficients is required. As an example, the off-the-shelf HS wavefront sensor from Thorlabs (item no. WFS150-5C) has an accuracy of $\lambda/15$ at 633 nm for the Zernike polynomial coefficients. Limit of detection (LOD) is the ratio between the minimal detectable value and the sensitivity of the value. LOD is calculated using Eq. (4) for any of the Zernike coefficients. For strictness of the calculation, we assume that the minimal detectable value of $R_m^0(r)$ (for $m = 0, 2, 4, 6$) coefficient is $\langle R_m^0(r)\rangle_{\min} = \lambda/10$

$$\mathrm{LOD} = \langle R_m^0(r)\rangle_{\min} / \mathrm{abs}\left[\frac{\partial R_m^0(r)}{\partial P}\right]. \tag{4}$$

Figure 8 depicts the sensitivity and LOD of the proposed device, with a thick membrane, in the pressure range of 12 to 40 mm Hg. For the first two coefficients $[R_0^0(r), R_2^0(r)]$, the LOD is less than 0.2 up to 40 mm Hg along with a moderate sensitivity, meaning that the minimal accuracy of the proposed device is ranging between 0.05 and 0.18 mm Hg in this range. While for the latter two coefficients, the LOD and sensitivity have a "jump" in values [since the change is not monotonic for $R_4^0(r)$ and the sensitivity is the absolute value of the derivative of $R_4^0(r)$] and high values [for $R_4^0(r)$ and $R_6^0(r)$].

Basically, there are three working regions of interest. First, the typical IOP ranging 12 to 21 mm Hg, second, at a medium pressure range of elevated IOP ranging 21 to 30 mm Hg, and the third region for pressures higher than 30 mm Hg. The first two regions cover the interesting area that is 12 to 30 mm Hg since pressures higher than 21 mm Hg re considered to be ocular hypertension, and for pressures higher than 30 mm Hg, treatment should be given immediately. Therefore, in the third region, the accuracy of the measurement is less important than the actual detection of the high level of pressure.

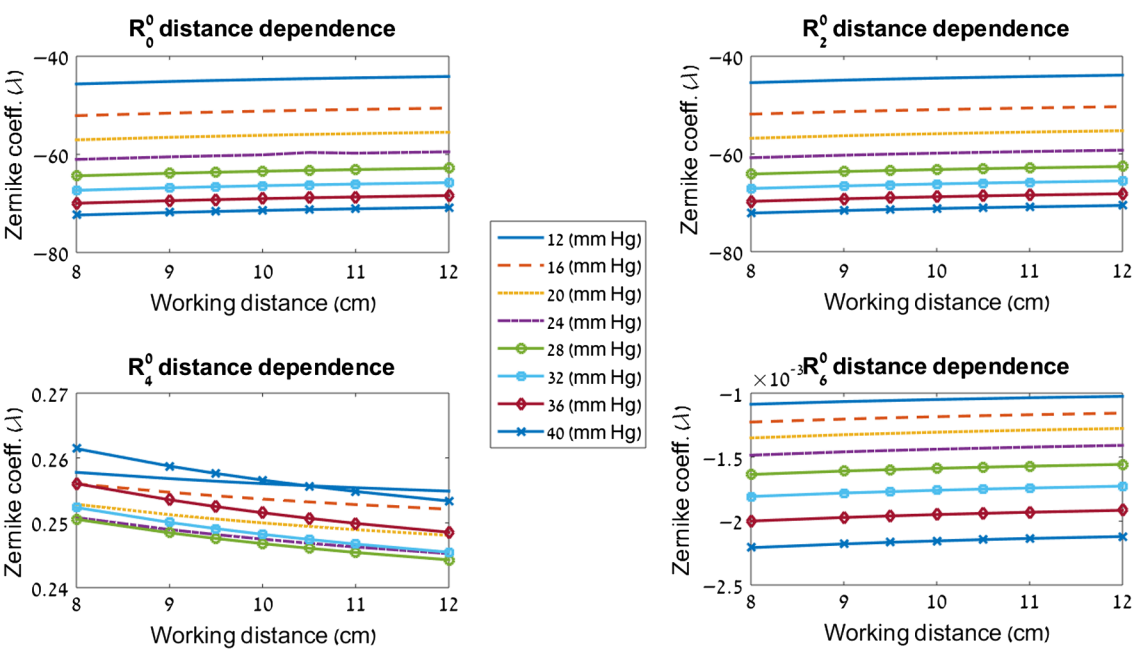

Fig. 7 Zernike polynomial coefficients distance dependence for various pressure values of a thick membrane.

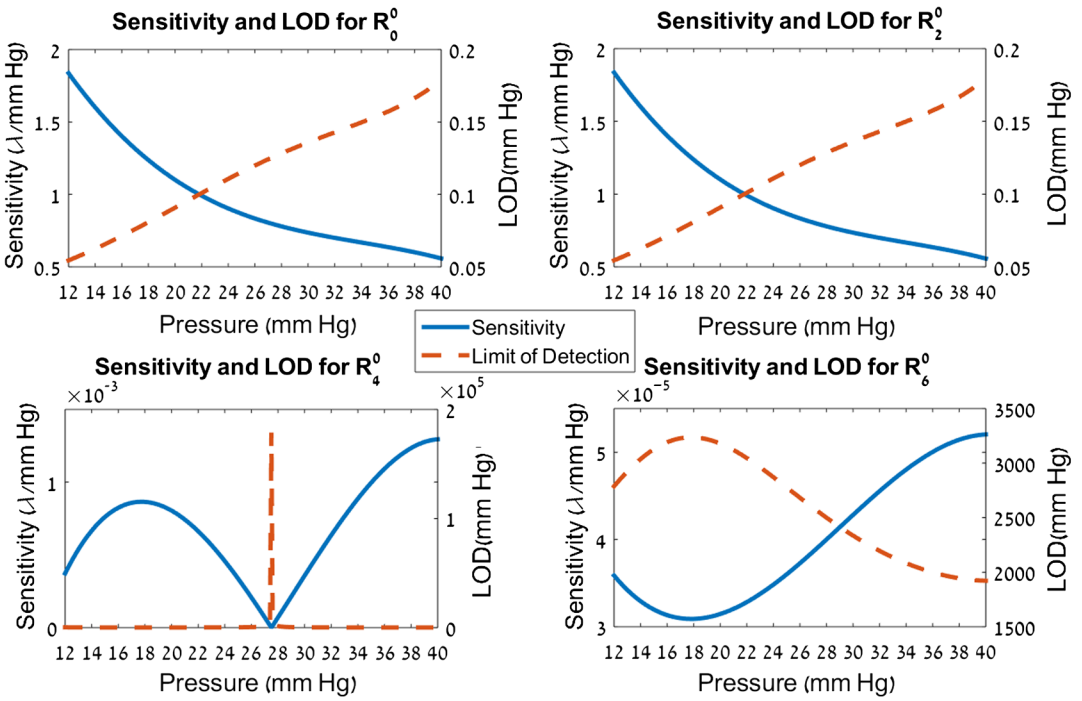

Fig. 8 Sensitivity and LOD of the proposed device, for a thick membrane, for four Zernike coefficients, and for pressure changes in the range of 12 to 40 mm Hg.

The minimal accuracy of the proposed device is ±0.2 mmHg in the first two regions and up to at least 40 mm Hg. Using a more accurate HS wavefront sensor would increase the accuracy of the device (for example, Thorlabs item no. WFS300-14AR has an accuracy of $\lambda/50$). It is important to state that even for an accuracy of $\lambda/4$ in the Zernike coefficient the LOD is acceptable for our purpose and will be less than ±0.5 mm Hg.

For proper examination of the proposed method, the sensitivity of the pressure to measurement distance may be calculated using the slopes calculated from Fig. 7 and the sensitivity of the Zernike coefficients to pressure (from Fig. 8). Figure 9 shows the pressure sensitivity that is in the range 0.2 to 0.7 mm Hg for a ±2 cm change around the working distance of 10 cm for $R_0^0(r)$, $R_2^0(r)$, $R_6^0(r)$, wherein for $R_4^0(r)$, the sensitivity is high

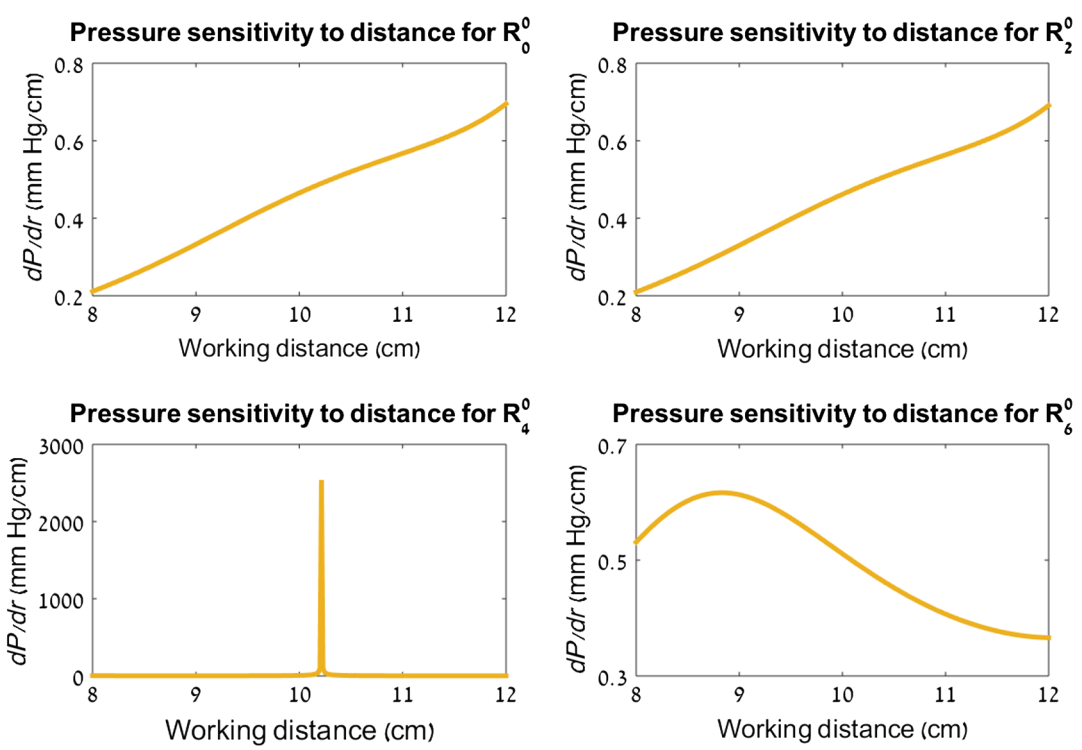

Fig. 9 Sensitivity of pressure to working distance of the four Zernike coefficients of a thick membrane.

Table 2 Summary of the theoretical study for the four contributing polynomials for a thick membrane. Note that $R_0^0(r)$ is not selected as appropriate because it represents the bias value of the wavefront.

	$R_0^0(r)$	$R_2^0(r)$	$R_4^0(r)$	$R_6^0(r)$
$R_m^0(r)$ distance dependence (λ/cm)	0.38 to 0.4	0.38 to 0.39	-9.7×10^{-4} to -1.2×10^{-3}	1.5×10^{-5} to 2.1×10^{-5}
Sensitivity (λ/mm Hg)	0.6 to 1.8	0.6 to 1.8	5.6×10^{-7} to 1.2×10^{-3}	3.1×10^{-5} to 5.2×10^{-5}
LOD (mm Hg)	0.05 to 0.18	0.05 to 0.18	77 to 1.8×10^{5}	1.9×10^{3} to 3.2×10^{3}
Pressure sensitivity to working distance (mm Hg/cm)	0.2 to 0.7	0.2 to 0.7	1.1 to 2.5×10^{3}	0.36 to 0.6
Suitable for IOP measurement	✗	✓	✗	✗

with a jump in values because of the nonmonotonic behavior of the coefficient. This singular point near 28 mm Hg is due to the extremum point in the sensitivity and we consider it as only mathematical as it occurs at one single point without physical meaning. The change is nearly linear with distance for the first two coefficients.

Although $R_0^0(r)$ and $R_2^0(r)$ are behaving the same in this case, $R_0^0(r)$ is the coefficient responsible for the intensity of the wavefront, wherein $R_2^0(r)$ is related to the parabolic shape of the membrane. Therefore, only $R_2^0(r)$ may be the most appropriate to use for IOP measurement.

In conclusion, for the thick membrane that was simulated and examined theoretically, it can be said that there is one Zernike polynomial, $R_2^0(r)$, that may be used to measure IOP with an accuracy less than 0.2 mm Hg and a distance dependence smaller than 0.7 mm Hg in the examined measurement distance. Table 2 summarizes the theoretical study for the four contributing polynomials for a thick membrane.

2.4.2 *Thin membrane*

The same steps in this section were performed as described in Sec. 2.4.1 for a membrane with $d = 100\,(\mu\text{m})$ and radius $R = 1000\,(\mu\text{m})$. These dimensions are the desirable dimensions for the final implanted device. Since the deformation will have the same shape, as shown in Ref. 18, we can conclude that the same polynomials would contribute to the deformation. The questions needed to be answered are whether we can use the same coefficients, and how is the contribution changed, if at all, after downscaling the membrane size. Since the same steps were used, we will present the figures for the new dimensions.

The solution obtained by COMSOL is presented in Fig. 10 for a PDMS membrane with $E = 1.12\,(\text{MPa})$, $\nu = 0.48$, thickness $d = 100\,(\mu\text{m})$, and radius $R = 1000\,(\mu\text{m})$.

Results for the four significant polynomials are described in Fig. 11. Out of the four polynomials, the first two $[R_0^0(r), R_2^0(r)]$

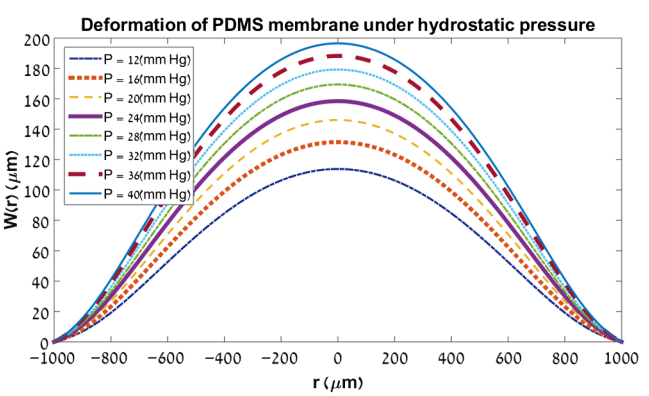

Fig. 10 Deformation of a PDMS membrane with $E = 1.12\,(\text{MPa})$, $\nu = 0.48$, $d = 100\,(\mu\text{m})$, and $R = 1000\,(\mu\text{m})$ for pressures in the range of 12 to 40 mm Hg.

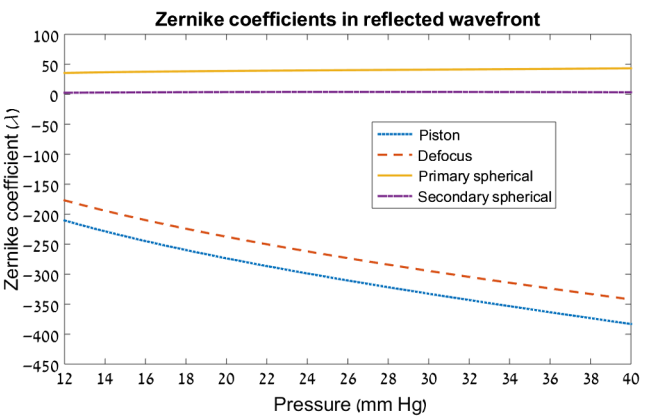

Fig. 11 Zernike coefficients for $R_0^0(r)$, $R_2^0(r)$, $R_4^0(r)$, and $R_6^0(r)$ (corresponding to piston, defocus, primary spherical, and secondary spherical, respectively) in the reflected wavefront for pressure changes in the range of 12 to 40 mm Hg.

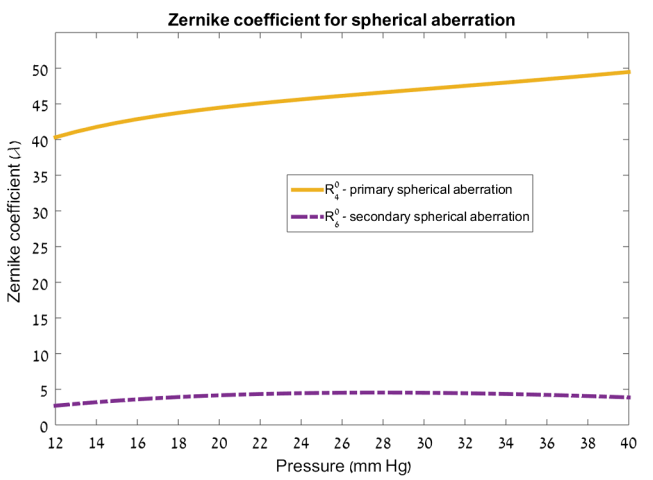

Fig. 12 Zernike coefficient for primary and secondary spherical aberration in the range of 12 to 40 mm Hg.

are greatly affected by the pressure and change with the measurement distance as in the thick membrane simulation, therefore, $R_2^0(r)$ may be used for IOP measurement [$R_0^0(r)$ is not used as explained in Sec. 2.4.1]. The last two polynomials $[R_4^0(r), R_6^0(r)]$ change when the membrane deforms (due to pressure changes), with a negligible dependence on the distance. Therefore, the last two polynomials may also be used, along with the coefficient found usable in Sec. 2.4.1, for IOP estimation.

The behavior of the Zernike coefficient for primary and secondary spherical aberration is described in Fig. 12. The monotonic behavior of R_4^0 suggests that the IOP can be estimated directly by measuring the Zernike coefficient for primary spherical aberration in the same way as R_2^0 was used. The change in R_6^0 is not monotonic, therefore, it cannot be used for IOP measurement.

Figure 13 describes the Zernike coefficients' distance dependence for various pressures. For the first two coefficients

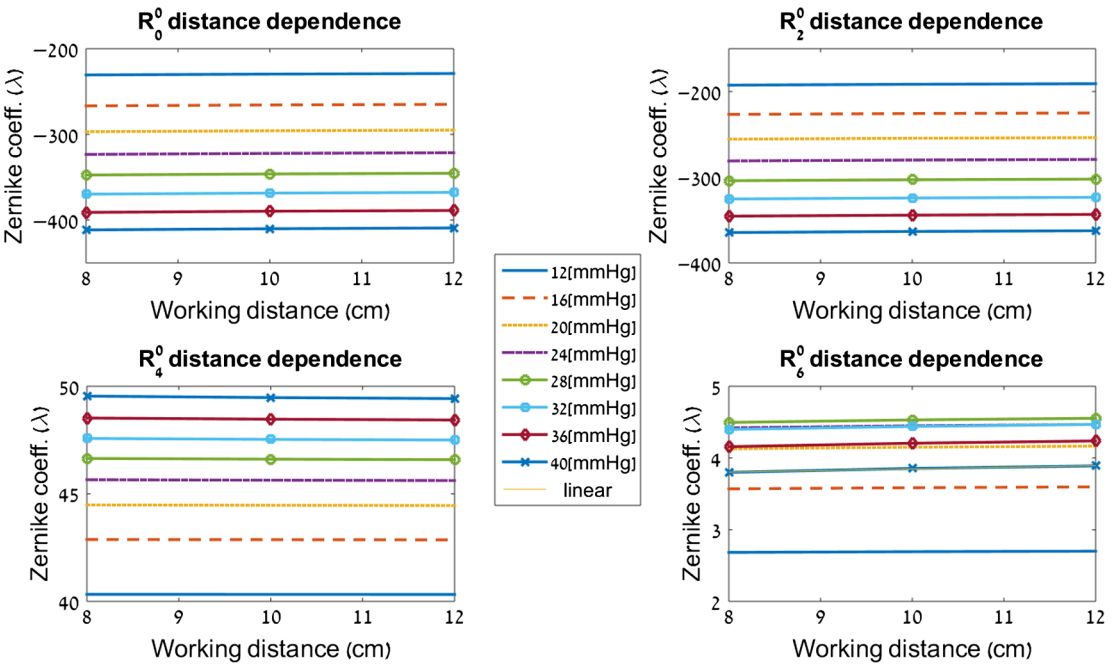

Fig. 13 Zernike polynomials distance dependence for various pressure values of a thin membrane.

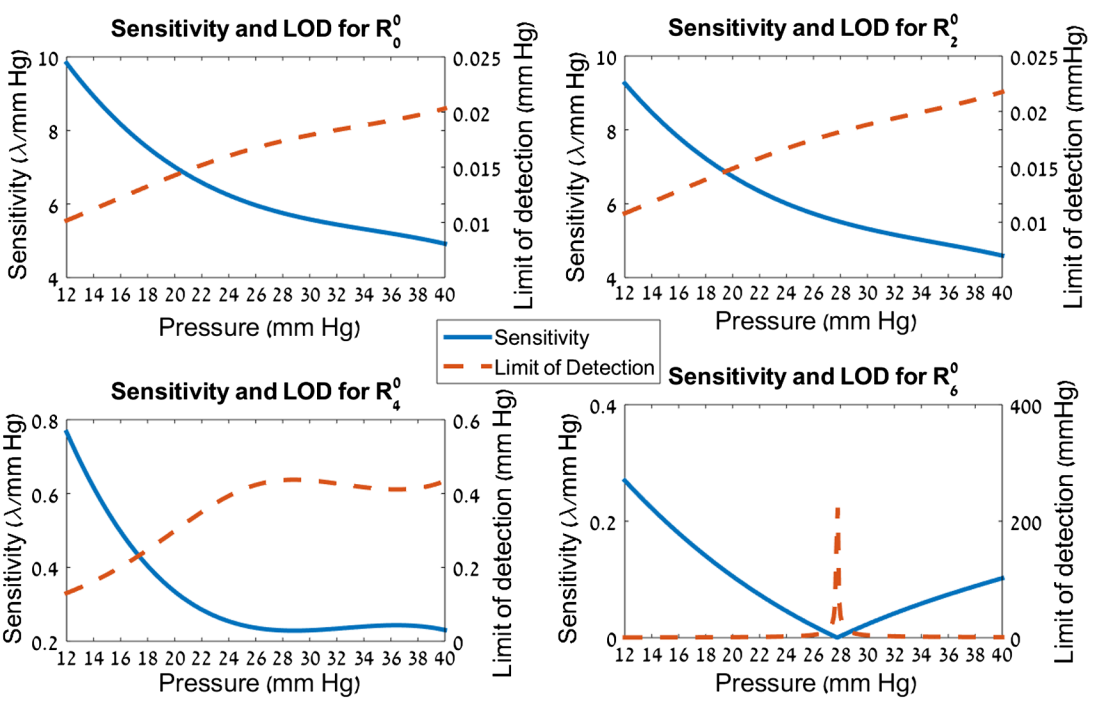

Fig. 14 Sensitivity and LOD of the proposed device, for a thin membrane, for four Zernike coefficients, for pressure changes in the range of 12 to 40 mm Hg.

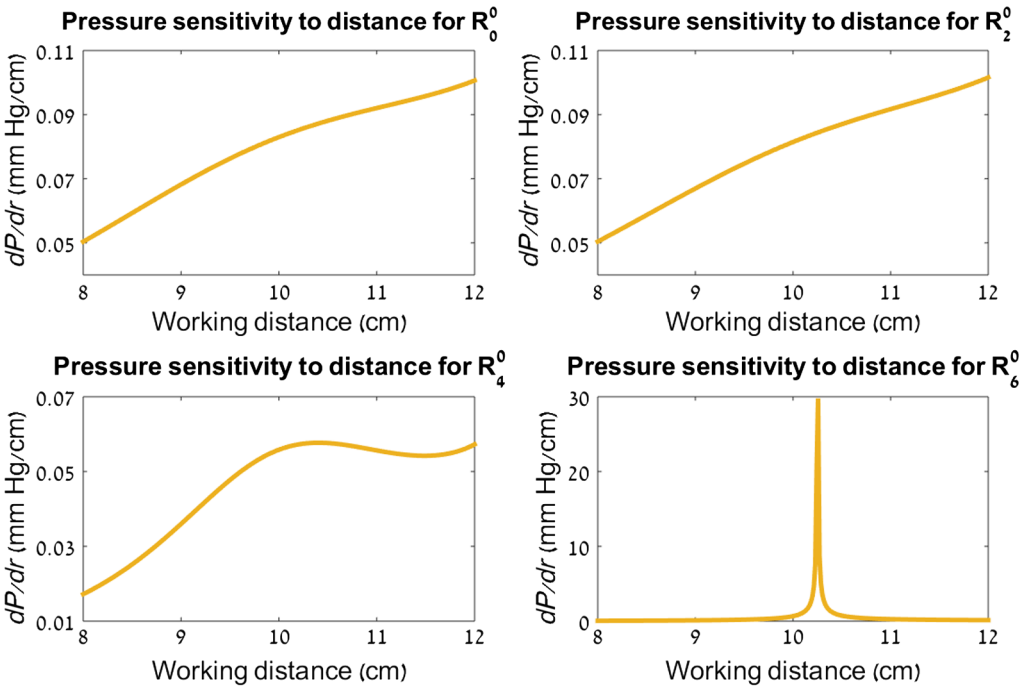

Fig. 15 Sensitivity of pressure to working distance of the Zernike coefficients of a thin membrane.

$R_0^0(r)$ and $R_2^0(r)$, the slope of the change is in the range of 0.4 to 0.5 λ/cm, while for $R_4^0(r)$ and $R_6^0(r)$, the slopes are −0.013 and 0.013 λ/cm, respectively.

Figure 14 depicts the sensitivity and LOD of the proposed device, with a thin membrane, in the pressure range of 12 to 40 mm Hg. For the first two coefficients, the LOD is less than 0.025 mm Hg up to 40 mm Hg along with very high sensitivity. For the latter two coefficients, the LOD is less than 0.45 for $R_4^0(r)$ and has high values for $R_6^0(r)$ (with a jump since the change is not monotonic as explained Sec. 2.4.1).

Figure 15 shows the pressure sensitivity that in the range 0.01 to 0.1 mm Hg for ±2 cm change around the working distance of 10 cm for $R_0^0(r)$, $R_2^0(r)$, $R_4^0(r)$, and for $R_6^0(r)$, the sensitivity is high with a jump in values because of the nonmonotonic behavior of the coefficient. The change is nearly linear with distance for the first two coefficients.

As stated in Sec. 2.4.1, $R_0^0(r)$ is the coefficient responsible for the intensity of the wavefront, wherein $R_2^0(r)$ is related to the parabolic shape of the membrane, therefore, $R_2^0(r)$ is suitable for IOP measurement. The difference from the thick membrane case is that $R_4^0(r)$ is affected by pressure and does not remain constant. Therefore, for a thin membrane, $R_2^0(r)$ and $R_4^0(r)$ both may be used for IOP measurement.

In conclusion, for the thin membrane that was simulated and examined theoretically and is the membrane size that is expected to be in the final device, it can be said that there are two Zernike polynomials, $R_2^0(r)$ and $R_4^0(r)$, that can be used to measure IOP with an accuracy less than 0.5 mm Hg. Table 3 summarizes the theoretical study for the four contributing polynomials for a thin membrane.

3 Experimental Demonstration

As a preliminary experiment, we designed and built an experimental setup with pressure conditions simulating the IOP as close as possible. To demonstrate the concept, we built a pressure chamber in which a PDMS membrane having the same thickness to radius ratio as in the simulations was clamped circularly and the pressure of a gas inside the chamber was changed gradually. Details of the experiment are given below.

Table 3 Summary of the theoretical study for the four contributing polynomials for a thin membrane. Note that $R_0^0(r)$ is not selected as appropriate because it represents the bias value of the wavefront.

	$R_0^0(r)$	$R_2^0(r)$	$R_4^0(r)$	$R_6^0(r)$
$R_m^0(r)$ distance dependence (λ/cm)	0.42 to 0.52	0.42 to 0.52	-7×10^{-3} to -2.8×10^{-3}	4×10^{-3} to 2.2×10^{-3}
Sensitivity (λ/mm Hg)	4.9 to 9.8	4.6 to 9.2	0.23 to 0.76	0 to 0.27
LOD (mm Hg)	0.01 to 0.02	0.01 to 0.02	0.13 to 0.43	0.37 to 223
Pressure sensitivity to working distance (mm Hg/cm)	0.05 to 0.1	0.05 to 0.1	0.02 to 0.57	0.05 to 29.8
Suitable for IOP measurement	✗	✓	✓	✗

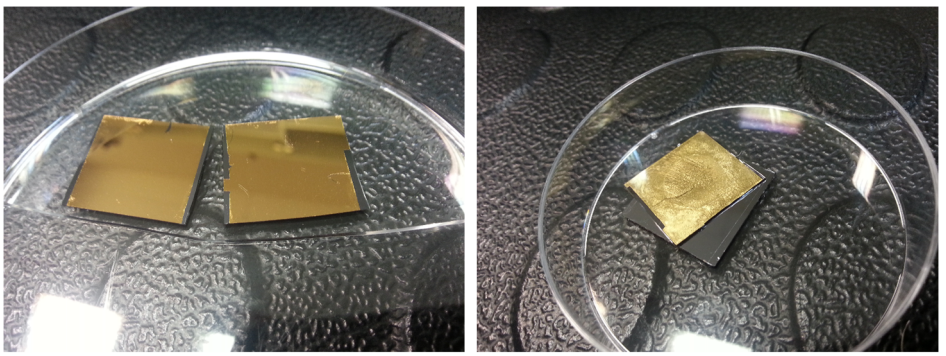

Fig. 16 (a) Cured PDMS poured over the coated Si wafer and (b) peeled off membrane.

3.1 *Reflective Membrane and Pressure Chamber Fabrication*

Production of the reflective membrane consisted of three stages. First, a metallic bilayer of Au (70 nm) and Ti (5 nm) was deposited on a clean silicon wafer by thermal evaporation. Then, PDMS was poured on top of the Ti film and cured in oven at 60°C for 1 h. Finally, the PDMS membrane was peeled off the wafer. Notably, the metallic layer easily detached from silicon due to both string adhesion of Ti to PDMS and poor adhesion of Au to silicon. The obtained membrane (Fig. 16) was ~0.5-mm thick and its active deformable diameter was ~10 mm to keep its ratio thickness-to-diameter ratio nearly the same as used in the simulation.

The fabricated membranes were characterized using a custom-made setup that consisted of a metallic pressure chamber with a acrylic window sealed with an elastomer O-ring [Fig. 17(a)] manufactured at Ben-Gurion University's mechanical workshop. Pressurized air was introduced into the chamber simulating the pressure build up in the human eye. The membrane was clamped circularly between two acrylic sheets with a hole in the center of a 10-mm diameter [see Fig. 17(b)]. A laser diode with a center wavelength of 660 nm and HS wavefront sensor (Thorlabs, WFS150-5C) were used to irradiate the deformed membrane and measure the deformed reflected wavefront. To measure the pressure difference between the chamber and the environment, a pressure gauge with an accuracy of ± 0.6 mm Hg (Extech, HD700) was connected to the chamber as well.

3.2 *Experimental Results*

The experiment was performed twice, using the same membrane reclamped again between the experiments. Repeatability of the results was examined as was the hysteresis of the setup. In the first set, three measurements were done [M1, M2, and hysteresis for M2 (decreased pressure from maximum point reached in measurement M2 down to atmospheric pressure)]; in the second set, five measurements were done (M3 to M7). The results are presented in Fig. 18. The zero of R_2^0 was taken for each curve as the value measured at 12 mm Hg and used as the reference for each measurement. We normalized all the measurements to examine the behavior of the Zernike coefficient with the change of pressure. This normalized form is presented in Fig. 19. The fact that there is a hysteresis behavior indicates the existence of gradients in the chamber, yet the effect is small and we can conclude that the Zernike coefficients are changing monotonically when pressure is increased or decreased, which is important for the functionality of the method. As can be seen in Fig. 18, there are changes between the different measurement sets and the sensitivity is lower than the expected theoretical one. However, the

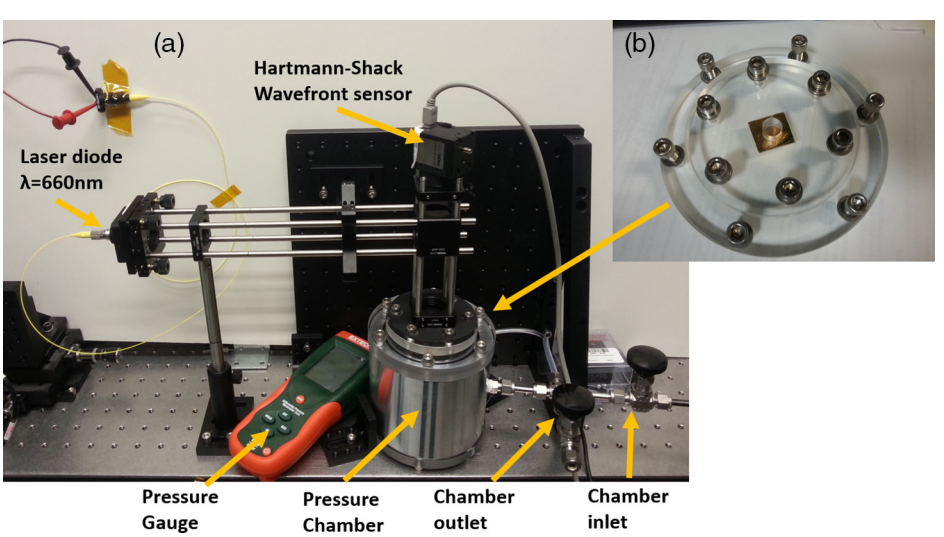

Fig. 17 (a) Experimental setup for measuring the deformation of the reflective membrane and (b) reflective membrane clamped between two acrylic sheets attached to the chamber cover.

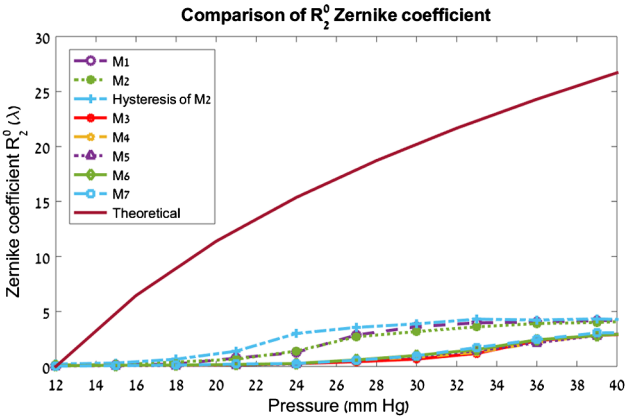

Fig. 18 Comparison of the theoretical values of Zernike coefficient for defocus and the measured values.

behavior is monotonic and the general trend is similar as can be seen from the normalized form presented in Fig. 19.

The measured values were stable when the power of the laser diode was changed (M1 was measured with low power and M2 was measured with high power). It can be seen that there is a smaller slope in the lower pressure region and differences between the two experiments. Although the ratio between the thickness and the diameter of the membrane is nearly the same and we expect to measure the values received in the simulation, the thick membrane may cause a deviation from the expected results. This may be explained by a residual stress present in the membrane before pressure is applied. When stress is present, the needed pressure for deformation is changing. Thick membranes can have a residual stress that can explain the delayed behavior observed at low-pressure values.[19] In our experiment, there are two more factors contributing to the stress present in the membrane. First, the clamping mechanism of the membrane causes inherent deformation. The membrane is clamped between two acrylic sheets and then tightened using six bolts. The gradual tightening results in uneven clamping of the membrane, and as a result, there are different forces at the edge of the membrane causing it to deform slightly immediately when clamped. With the naked eye, we could see a deformation having an asymmetrical shape that can cause a delay in the deformation. Since there are forces acting on the membrane because of the clamping, higher pressure values

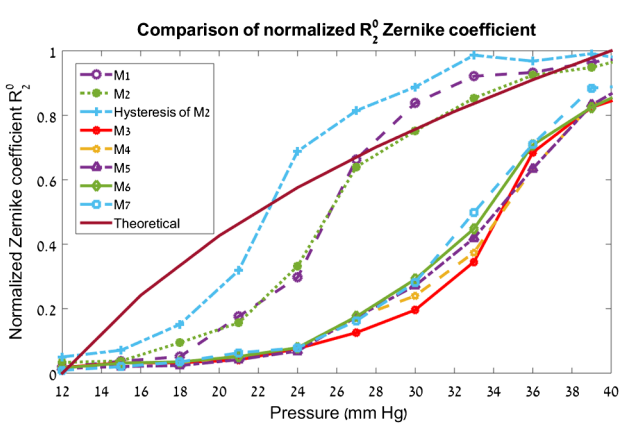

Fig. 19 Comparison of the normalized forms of the theoretical values of Zernike coefficient for defocus and the measured values.

are needed to overcome these forces and start the gradual deformation. To measure the deformation and achieve the expected results that were seen in the simulation, the PDMS membrane should perhaps be adhered to the acrylic and not clamped. This has not been achieved in our lab yet since there is an adhesion problem of PDMS to other materials. Another possible cause for the discrepancy is the gravitational force acting on the relatively thick membrane and causing it to deform in the opposite direction of the pressure action. All these aspects were not taken into account in the simulation and might definitely affect the mechanism and explain the discrepancy observed.

Since the membrane is deformable, cracks appear in the reflective layer. To prevent these cracks, one concept is not to have the layer continuously uniform but rather composed of a pillar structure where the ends of the pillars are reflecting and the gaps between them are filled with the PDMS without coating. See Ref. 20 for the manufacturing process. The main concern with this solution is that this is a metallic grating and surface plasmons or diffraction resonances may appear. If the grating size and the pitch are chosen correctly, these resonances will not appear for the wavelength used and will not affect the measurement. For example, we checked by simulations that an Au grating of 20 μm lines width with a period of 24 μm will not give a resonance for the wavelength range 400 to 800 nm.

In the final implementation of the method, we suggest that instead of using a commercial HS wavefront sensor, a microlens array combined with a mobile phone (or a CMOS sensor) can be used to act as a low cost and handy HS wavefront sensor, similar to what was done by Pamplona et al.[21] or by Nirmaier et al.[22]

4 Summary

A flexible reflective membrane was suggested as a basis of an IOP measurement optical device. The structure of the device was simulated and its response to pressure changes was examined, leading to the conclusion that it can provide an optical passive IOP measurement device. Using an HS wavefront sensor and Zernike decomposition, such a device can provide a measurement resolution of less than ± 0.2 mm Hg with a pressure dependence on a working distance less than 0.7 mm Hg/cm for a thick membrane. The resolution for a thin membrane is ± 0.45 mm Hg with a pressure dependence on a working distance less than 0.6 mm Hg/cm.

A preliminary experimental validation of this method was performed for the simulation of the thick membrane, in which we observed that the values for R_2^0 are changing monotonically and they are stable and repeatable. Improvements on the experiment are required to get a more quantitative agreement with the simulations, for example, by choosing thinner membranes, better clamping of the membrane, and looking for better methods of membrane adherence.

It is important to note that the results might be improved further by using a slightly different elastomeric material that responds more strongly to pressure changes and increases the accuracy of the proposed method. Also, using a more accurate HS wavefront sensor should increase the accuracy of the device.

Disclosures

No conflicts of interest, financial or otherwise, are declared by the authors.

Acknowledgments

The authors would like to thank Dr. Michael Ney, Yossi Keydar, and Avichai Marcovitch for the useful discussions, suggestions, and help. Andrey Nazarov performed the simulations, design, and experiment, Professor Tova Lifshitz and Dr. Boris Knyazer proposed the IOP measurement problem and the possibility of implanting the IOP sensor in the AC or the cornea, Dr. Mark Schwartzman advised on the fabrication process of the mirror, and Professor Abdulhalim proposed the deformable mirror concept and supervised the whole project. All authors contributed to the writing of the paper.

References

1. S. Kingman, "Glaucoma is second leading cause of blindness globally," *Bull. World Health Org.* **82**(11), 887–888 (2004).
2. Y.-C. Tham et al., "Global prevalence of glaucoma and projections of glaucoma burden through 2040: a systematic review and meta-analysis," *Ophthalmology* **121**(11), 2081–2090 (2014).
3. H. A. Quigley and A. T. Broman, "The number of people with glaucoma worldwide in 2010 and 2020," *Br. J. Ophthalmol.* **90**(3), 262–267 (2006).
4. D. Piso, P. Veiga-Crespo, and E. Vecino, "Modern monitoring intraocular pressure sensing devices based on application specific integrated circuits," *J. Biomater. Nanobiotechnol.* **3**(2A), 301–309 (2012).
5. Y. Backlund et al., "Passive silicon transensor intended for biomedical, remote pressure monitoring," *Sens. Actuators A* **21**(1–3), 58–61 (1990).
6. E. Y. Chow, A. L. Chebowski, and P. Irazoqui, "A miniature-implantable RF-wireless active glaucoma intraocular pressure monitor," *IEEE Trans. Biomed. Circuits Syst.* **4**(6), 340–349 (2010).
7. C. Varel et al., "A wireless intraocular pressure monitoring device with a solder-filled microchannel antenna," *J. Micromechan. Microeng.* **24**(4), 045012 (2014).
8. P. Auvray et al., "A passive pressure sensor for continuously measuring the intraocular pressure in glaucomatous patients," *IRBM* **33**(2), 117–122 (2012).
9. M. Leonardi et al., "Wireless contact lens sensor for intraocular pressure monitoring: assessment on enucleated pig eyes," *Acta Ophthalmol.* **87**(4), 433–437 (2009).
10. T. Karrock and M. Gerken, "Pressure sensor based on flexible photonic crystal membrane," *Biomed. Opt. Express* **6**(12), 4901–4911 (2015).
11. L. Fu et al., "A pressure sensor based on the orientational dependence of plasmonic properties of gold nanorods," *Nanoscale* **7**(34), 14483–14488 (2015).
12. Y. Nazirizadeh, T. Karrock, and M. Gerken, "Visual device for pressure measurement using photonic crystal slabs," *Opt. Lett.* **37**(15), 3081–3083 (2012).
13. X. Zhang et al., "Soft plasmons with stretchable spectroscopic response based on thermally patterned gold nanoparticles," *Sci. Rep.* **4**, 4182 (2014).
14. European Glaucoma Society, *Terminology and Guidelines for Glaucoma*, 3rd ed., Editrice DOGMA S.r.l., Savona, Italy (2008).
15. J. A. Goldsmith et al., "Anterior chamber width measurement by high-speed optical coherence tomography," *Ophthalmology* **112**(2), 238–244 (2005).
16. S. P. Timoshenko and S. Woinowsky-Krieger, *Theory of Plates and Shells*, 2nd ed., p. 402, Mcgraw-Hill College, New York (1959).
17. S. T. Choi et al., "Opto-mechanical analysis of nonlinear elastomer membrane deformation under hydraulic pressure for variable-focus liquid-filled microlenses," *Opt. Express* **22**(5), 6133–6146 (2014).
18. A. Nazarov and I. Abdulhalim, "Universal form of the equations governing membrane deformation under hydrostatic pressure for simpler design of sensors and tunable optical devices," *Sens. Actuators A* **257**, 113–117 (2017).
19. W. K. Schomburg, "Membranes," in *Introduction to Microsystem Design*, 2nd ed., pp. 43–71, Springer, Berlin, Heidelberg (2015).
20. S. Ghassemi et al., "Gold-tipped elastomeric pillars for cellular mechanotransduction," *J. Vac. Sci. Technol. B* **6**, 3088–3091 (2009).
21. V. F. Pamplona et al., "Dual of Shack–Hartmann optometry using mobile phones," in *Frontiers in Optics 2010/Laser Science XXVI, OSA Technical Digest*, Optical Society of America (2010).
22. T. Nirmaier, G. Pudasaini, and J. Bille, "Very fast wave-front measurements at the human eye with a custom CMOS-based Hartmann–Shack sensor," *Opt. Express* **11**(21), 2704–2716 (2003).

Andrey Nazarov is an MSc student of Electro-Optic Engineering at the Ben-Gurion University (BGU) of the Negev. He received his BSc degree in physics from the Hebrew University of Jerusalem in 2011. His current research interest is in intraocular measurement techniques. He is a member of the SPIE student chapter at BGU.

Boris Knyazer has finished the Goldman Medical School, Ben-Gurion University (BGU), Beer-Sheva, Israel, in 2005 and completed his residency in the Ophthalmology Department at the Soroka University Medical Center (SUMC) in 2011. He is a senior consultor and surgeon with professional interest to diseases of anterior segment of the eye, cataract and laser refractive surgery, and corneal transplantation. Currently, he is the director of ophthalmology clinics in SUMC and lecturer in BGU. He has 30 publications in peer-reviewed literature.

Tova Lifshitz has graduated Sackler Medical School, Tel-Aviv, Israel, in 1978. She is a chief in the Ophthalmology Department at the Soroka University Medical Center (SUMC), Beer-Sheva, Israel. Her professional interest is diseases of anterior segment of the eye, cataract and laser refractive surgery, and corneal transplantation. She is a full clinical professor at the Ben-Gurion University of the Negev, Beer-Sheva, Israel. She has published over 100 papers in ophthalmology peer-reviewed literature and several medical patents.

Mark Schvartzman received his bachelor's degree and master's degree from the Technion and his PhD from Columbia University. Following a period of postdoctoral training in Weizmann Institute, he joined the Department of Materials Engineering in the Ben-Gurion University of the Negev as a faculty member in 2014. His main research interests are ultrahigh resolution nanolithography and nanofabrication, and their applications in bottom-up nanoelectronics, nanophotonic structures, and biointerfaces.

Ibrahim Abdulhalim is a professor in the Department of Electro-Optic Engineering at Ben-Gurion University since 2005. His current research involves liquid crystal devices, nanophotonic and plasmonic biosensors, and improved biomedical optical imaging techniques. He has published over 160 papers, 10 book chapters, coauthored two books, and has over 15 patents. He is a fellow of the IoP and the SPIE. He is an associate editor of the SPIE Journal of Nanophotonics.